VI CONGRESSO NACIONAL DE ENGENHARIA MECÂNICA
VI NATIONAL CONGRESS OF MECHANICAL ENGINEERING
18 a 21 de agosto de 2010 – Campina Grande – Paraíba - Brasil
August 18 – 21, 2010 – Campina Grande – Paraíba – Brazil

AIRCRAFT GROUND DYNAMICS MODELING

CON10-1827

Abstract. *Along the years, air traffic has increased significantly and in order to accommodate this, new technologies were developed for all flight phases, from taking off to landing, maximizing efficiency on air. In this context, ground operation became the bottle neck of all aircraft operation, since it is highly based on non-automatic operations and human interaction. To increase efficiency, optimal ground trajectory generation and tracking by aircraft needed to be developed. For tracking, mathematical models are necessary. This paper proposes a five degree of freedom model for aircraft ground dynamics, assuming aircraft as a rigid body. The model takes into account the landing gear, tires, brakes, propulsion, aerodynamic efforts and associated moments. Most efforts are modeled in a non-linear way, based on components, physical construction, typical values / curves and classic calculations, which were provided by specific literature. Besides the model itself, a simple speed control law is proposed, which takes into consideration typical ground operations and speed profiles. Simulation and responses over time were performed and they are presented as well.*

Keywords: *Aircraft ground dynamics, Aircraft modeling*

1. INTRODUCTION

In last years, the number of flights around the world suffered an expressive growth. To deal with this, several technologies were developed to increase efficiency in all flight phases: take off, cruise, loiter and landing. In this scenario, taxiing operations became the weak point of all operation since it is highly dependent on human spoken communication and actions. The last researches point out that ground efficiency depends on keeping the aircraft the minimum time in runaways and taxiways, to allow the maximum possible use of these spaces. To perform this task, the first approach is to generate optimum trajectories, taking into account the free spaces and the quantity of aircrafts on ground. Once the trajectories are defined in some instant of time, the natural step is following these paths in an automatic way, providing suitable tracking. This approach has two direct consequences: a mathematical model of the aircraft on ground is needed, and control laws are necessary.

Very few references can be found on this subject. Some approaches (Coetzee, et al., 2006) focus on stability using sophisticated non-linear tools. Other works (Duprez, et al., 2004a) and (Duprez, et al., 2004b) propose simple 3 degree of freedom models and a dynamic inversion as control law. A similar approach was developed by (Goto, et al., 2001) and validated with tests results. In all approaches, the mathematical model itself is just highlighted, and more details are provided about contro law.

As a suggestion for this lack of information, this paper proposes a five degree of freedom mathamatical model. Aspects from several agents of ground dynamics are considered, such as landing gear, tires, engines, brakes and some aerodynamic efforts. As a complement, a simple control law for speed is proposed, taken into account a typical expected ground operation.

2. MATHEMATICAL MODELING

The mathematical modeling was divided into two different parts: aircraft general equations and components / efforts modeling. Both aspects will be discussed in next sections.

2.1. Aircraft General Equations

The mathematical model was developed considering the aircraft as a rigid body. The basic physics that govern all the movement can be found on (Etkin, et al., 1996). Two frames of reference are defined: one earth-fixed frame

$F_e(O_e, x_e, y_e, z_e)$, considered as inertial referential and a second frame $F_b(O_b, x_b, y_b, z_b)$ docked on aircraft CG. Frames orientation can be found on Fig. 1.

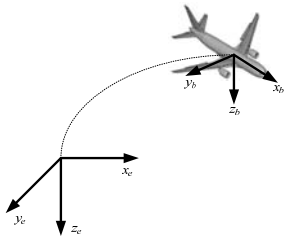

Figure 1 - Reference frames

With the frames defined, the general equations can be derived. They are a classical application of second Newton's law to a rigid body complemented with kinematic equations, obtained from Euler's angles and geometrical considerations. Applications of Newton's law are described in Eq. (1) and Eq. (2).

$$M_b = I_b \cdot \frac{d\omega_b}{dt} + \omega_b \times I_b \cdot \omega_b \quad (1)$$

$$F_b = m \cdot \left(\frac{dV_b}{dt} + \omega_b \times V_b \right) \quad (2)$$

With

$\omega_b = [p \quad q \quad r]^T$	Angular velocity vector of $\boldsymbol{F_b}$ around $\boldsymbol{F_e}$ expressed in $\boldsymbol{F_b}$ coordinates
$V_b = [u_b \quad v_b \quad w_b]^T$	Velocity vector of $\boldsymbol{F_b}$ related $\boldsymbol{F_e}$ expressed in $\boldsymbol{F_b}$ coordinates
$M_b = [L_{Res} \quad M_{Res} \quad N_{Res}]^T$	Moments vector applied to body expressed in $\boldsymbol{F_b}$ coordinates
$F_b = [X_{Res} \quad Y_{Res} \quad Z_{Res}]^T$	Forces vector applied to body expressed in $\boldsymbol{F_b}$ coordinates
I_b, m	Inertia tensor in $\boldsymbol{F_b}$ coordinates and body mass

2.2. General Data

Based on reference data provided by (Embraer, 2008) and reproduced on Fig. 2, a scaled CAD drawing was developed, to obtain some reference parameters used for modeling. The most important ones are the reference wing area (S), the dihedral angle, the quarter chord angle ($\Lambda_{c/4_W}$) and the wingspan (b) and are written in Tab. 1.

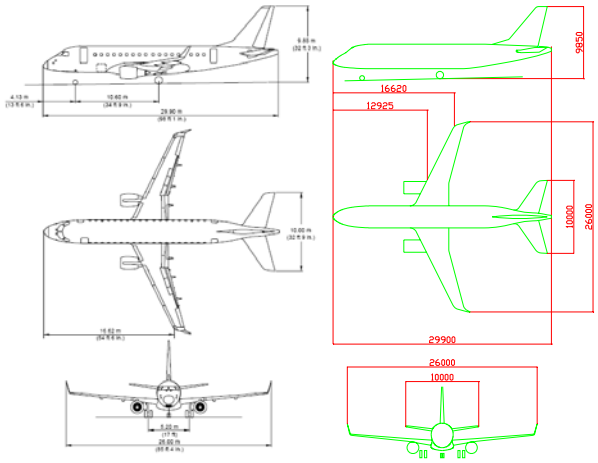

Figure 2 - Reference and scaled drawing

Parameter	Value	Unit
$\Lambda_{c/4_W}$	24	[°]
diedral angle	5	[°]
S	72,72	$[m^2]$
b	25	$[m]$

Table 1 - Aircraft basic parameters

According to the document (Embraer, 2008), the CG travel was obtained to be used in modeling, especially landing gear. Based on this information, the aircraft operation point was defined as the Maximum Lading Weight (32800 kgf), mean CG (17 % Mean Aerodynamic Chord) location and initial speed of 72,0222 m/s (140 knot), a typical landing speed.

2.3. Landing Gear Modeling

The considered landing gear was a tricycle type, the most common configuration used nowadays. It was modeled taking into consideration three different aspects: lateral efforts, brakes and free wheel friction and vertical forces. For all of them, some distances (mainly from CG) were considered, according to Fig. 3.

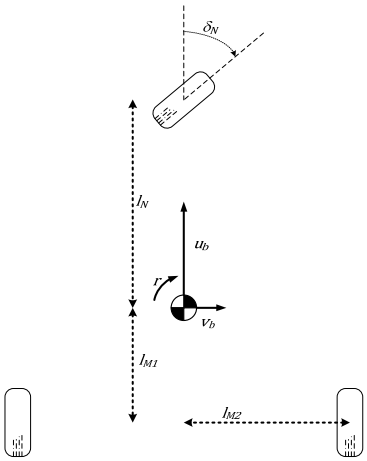

Figure 3 - Definitions for landing gear

2.3.1. Lateral Efforts

The lateral efforts in landing gears are the forces that allow aircraft maneuvering on ground. They are a direct consequence of the tire / runaway interaction. Lateral forces are modeled as function of two variables: lateral friction coefficient μ and vertical load on tire Z. The first one in a function of speed V, the vertical load Z and the sideslip angle α, defined as the difference between tire longitudinal axis and speed vector. The nose wheel deflection is a variable in the system. Using the definitions of Fig. 4, the slip angles for three tires can be defined according to Eq. (3), Eq. (4) and Eq. (5).

$$\alpha_N = \delta_N - tan^{-1}\left(\frac{v_b + r \cdot l_N}{u_b}\right) \quad (3)$$

$$\alpha_{M_l} = tan^{-1}\left(\frac{v_b - r \cdot l_{M_1}}{u_b + r \cdot l_{M_2}}\right) \quad (4)$$

$$\alpha_{M_r} = tan^{-1}\left(\frac{v_b - r \cdot l_{M_1}}{u_b - r \cdot l_{M_2}}\right) \quad (5)$$

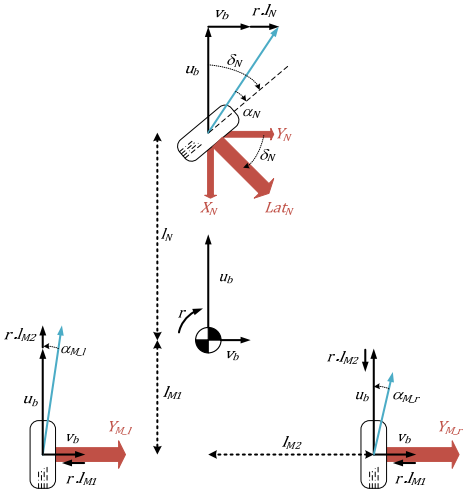

Figure 4 - Landing gear lateral forces

The lateral force for each tire can be evaluated according to Eq. (6) and Eq. (7) for nose landing gear and Eq. (8) and Eq. (9) for main landing gear. Notice that no angle was taken into account for main landing gear force direction, since a small value is expected for this parameter.

$$Y_{N_{Lat}} = \mu(\alpha_N, Z_N, V) \cdot Z_N \cdot \cos(\delta_N) \quad (6)$$

$$X_{N_{Lat}} = \mu(\alpha_N, Z_N, V) \cdot Z_N \cdot \sin(\delta_N) \quad (7)$$

$$Y_{M_{l_{Lat}}} = -\mu(\alpha_{M_l}, Z_{M_l}, V) \cdot Z_{M_l} \quad (8)$$

$$Y_{M_{r_{Lat}}} = -\mu(\alpha_{M_r}, Z_{M_r}, V) \cdot Z_{M_r} \quad (9)$$

The non linear relations expressed by the equations above were obtained from (Yaeger, et al., 1990). The basic information from reference was adjusted to the aircraft category object of this study. The final curves can be seen on Fig. 5.

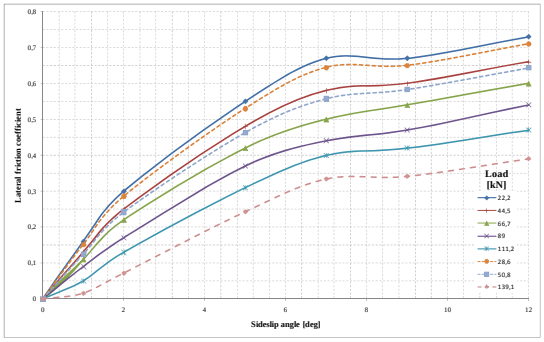

Figure 5 - Lateral friction coefficient curves

The moments associated with the forces are expressed from the correlation between the forces previously calculated and the distances from Fig. 3, provided by Eq. (10) to Eq. (12).

$$N_{N_{Lat}} = Y_{N_{Lat}} \cdot l_N \quad (10)$$

$$-N_{M_{l_{Lat}}} = Y_{M_{l_{Lat}}} \cdot l_{M_l} \quad (11)$$

$$-N_{M_{r_{Lat}}} = Y_{M_{r_{Lat}}} \cdot l_{M_l} \quad (12)$$

2.3.2. Vertical Forces

Vertical forces act during the landing, absorbing the vertical kinetic energy of the aircraft as represented in Fig. 6. In this modeling, an oleo pneumatic landing gear was considered. In this type of landing gear, a gas inside the shock absorber causes the spring effect, while the oleo passing through an orifice acts as damper. As a consequence, a simple spring-damper model was considered for main and nose landing gear. The spring effect is non-linear, and it was calculated according to the bases design methodology proposed by (Currey, 1988), using as input data information from (Agência nacional de aviação civil, 2009).

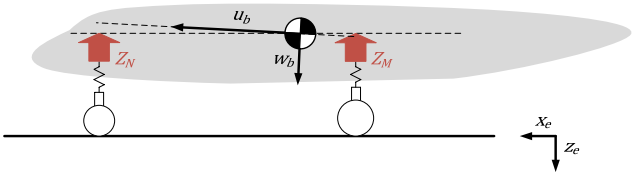

Figure 6 - Landing gear vertical forces

Figure 7 provides the final deflection x force curves (spring effect) for each landing gear, and the damper coefficient can be seen on Tab. 2.

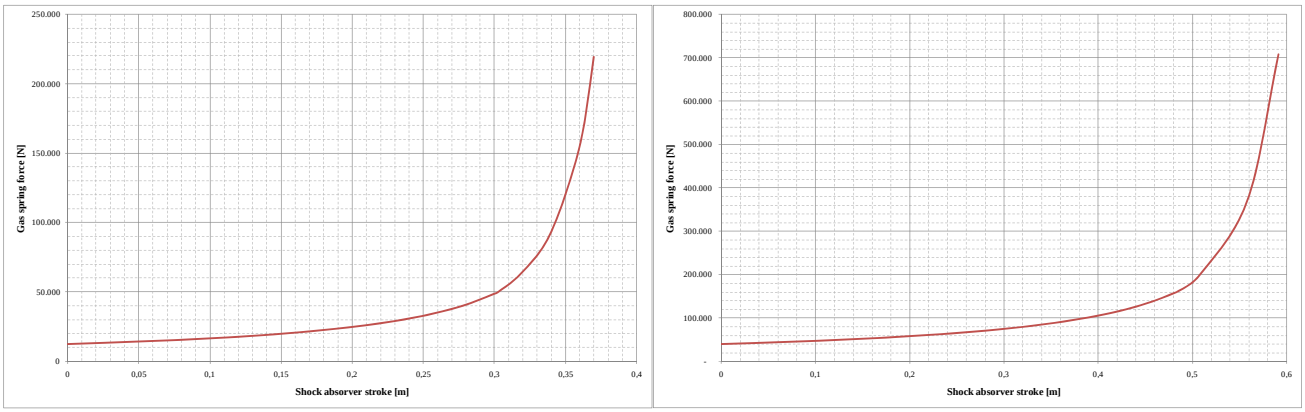

Figure 7 - Force x deflection curves - nose and main landing gear

	Damping coefficient	Unit
Nose landing gear	$damp_N$=410.062.378	$\left[\frac{N}{m^2/s^2}\right]$
Main landing gear	$damp_M$=31.286.322	$\left[\frac{N}{m^2/s^2}\right]$

Table 2 - Damping coefficient for nose and main lading gear

2.3.3. Brakes and Free Wheel Friction

Brake forces X_{M_B} are the forces that act in the aircraft making it to stop during landing or rejected take off. They were modeled as a control signal $\pi_B \in [0,1]$ multiplied by a dynamics and a maximum deceleration value selected as $-4 \cdot m$,according to (Roskam, 2000). The dynamic was adjusted to provide a low-pass frequency response with cutting frequency of 5 Hz, a typical value in aircraft braking systems. They were considered only in main landing gears. The final form of this force is provided by Eq. (13).

$$X_{M_B} = \pi_B \cdot \frac{1}{3 \cdot 10^{-2} \cdot s + 1} \cdot 4 \cdot m \qquad (13)$$

Free wheel forces Fw are the deceleration efforts that naturally occur in a tire running on a runaway. They are proportional to a tire-runway friction, considered as 0,05 according to (Roskam, 2000) and to vertical load Z applied to the tire. These forces always act in tire longitudinal axis direction, leading to a lateral force in nose landing tire when this is subjected to a deflection. Figure 8 clarify these concepts and Eq. (14), Eq. (15) and Eq. (16) detail the mathematical description for free wheel force in each tire.

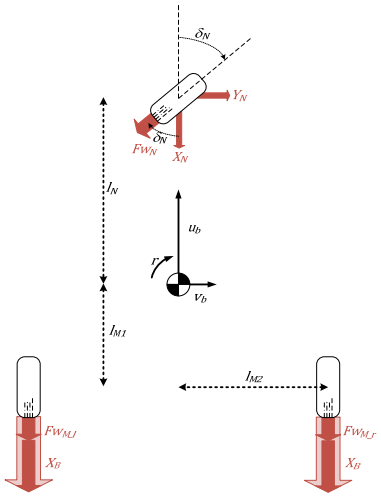

Figure 8 - Brake and free wheel forces

$$Y_{N_{Fw}} = -Z_N \cdot \mu_B \cdot sin(\delta_N) \quad (14)$$
$$X_{N_{Fw}} = Z_N \cdot \mu_B \cdot cos(\delta_N) \quad (15)$$
$$X_{N_{Fw}} = Z_M \cdot \mu_B \quad (16)$$

These forces can be grouped as horizontal forces Y_H and X_H, according to Eq. (17) and Eq. (18).

$$Y_H = Y_{N_{Fw}} \quad (17)$$
$$X_H = X_{N_{Fw}} + X_{M_B} + X_{M_{Fw}} \quad (18)$$

Moments associated with horizontal forces are described by Eq. (19) and Eq. (20)

$$N_H = Y_H \cdot l_N \quad (19)$$
$$-M_H = X_H \cdot z \quad (20)$$

2.4. Aerodynamic Modeling

Only rudder aerodynamic effects were considered in this modeling because the aircraft was assumed in a landing situation, when ground spoilers were deployed and no lift was generated by wing. A classical approach was considered with the assumption that aerodynamic efforts are linear related to some interest variables (sideslip angle β, rudder deflection δ_r and yaw rate r), according to Eq. (21) to Eq. (26). All efforts are proportional to speed V and air density ρ. An important point is that parameter δ_r is a variable control , responsible to gather the nose wheel deflection by aircraft maneuvers on ground.

$$Y_r = \frac{1}{2} \cdot \rho \cdot V^2 \cdot S \cdot C_{Y_r} \cdot r \quad (21)$$
$$N_r = \frac{1}{2} \cdot \rho \cdot V^2 \cdot S \cdot b \cdot C_{Y_r} \cdot r \quad (22)$$
$$Y_{\delta_r} = \frac{1}{2} \cdot \rho \cdot V^2 \cdot S \cdot C_{Y_{\delta_r}} \cdot \delta_r \quad (23)$$
$$N_{\delta_r} = \frac{1}{2} \cdot \rho \cdot V^2 \cdot S \cdot b \cdot C_{N_{\delta_r}} \cdot \delta_r \quad (24)$$
$$Y_\beta = \frac{1}{2} \cdot \rho \cdot V^2 \cdot S \cdot C_{Y_\beta} \cdot \beta \quad (25)$$
$$N_\beta = \frac{1}{2} \cdot \rho \cdot V^2 \cdot S \cdot b \cdot C_{N_\beta} \cdot \beta \quad (26)$$

The parameters C_{Y_r}, C_{Y_r}, $C_{Y_{\delta_r}}$, $C_{N_{\delta_r}}$, C_{Y_β} and C_{N_β} were defined according to the classical methodology proposed by (Roskam, 2000), using geometrical considerations about the aircraft in study. Final values can be seen in Tab. 3.

Parameter	Value	Unit
C_{Y_β}	-0,65527	-
$C_{Y_{\delta_r}}$	0,286935	-
C_{Y_r}	0,023184	-
C_{N_β}	0,232688	-
$C_{N_{\delta_r}}$	-0,14479	-
C_{N_r}	-0,2077	-

Table 3 - Aerodynamic parameters

2.5. Propulsion Modeling

The propulsion was modeled quite similar to brakes. A control signal $\pi_P \in [0,1]$was multiplied by a maximum thrust value, obtained from (Embraer, 2008) as 62.300 N and a dynamics that simulates the typical 5~10 s delay in engine response after a command. Overall expression can be seen on Eq. (27).

$$X_{M_P} = \pi_P \cdot \frac{0,15}{s+0,15} \cdot 62300 \quad (27)$$

No moments around y_b axis, due to propulsion, were considered in this modeling. This is reasonable to assume in the selected operation point, since propulsion is expected to be minimum. Besides, the distance between aircraft CG and engines are significantly smaller than the brakes one.

3. SPEED CONTROL LAW

In a real aircraft, the speed on ground is controlled through the thrust and brakes. On landing operations, aircraft touches the ground with engines in almost minimum power; just enough to avoid aircraft stall. Once on ground, the engine is kept to a minimum whilst brakes are used mainly.

In this study, the control of brakes and propulsion was done separately, in such a way that no brakes and propulsion were applied at the same time. This is not fully compatible with the possibilities of a real aircraft, but is a valid simple approach for landing operations according to the discussion above. For both controls, a controller $G(s) = K_p + \frac{K_i}{s+p}$ was selected. The objective was following the reference speed V_r, defined according to typical landing values in real operations. The *Cumbica* airport (placed at Guarulhos, Brazil) was selected as reference airport. According to Fig. 9, the yellow line is the selected trajectory on the airport.

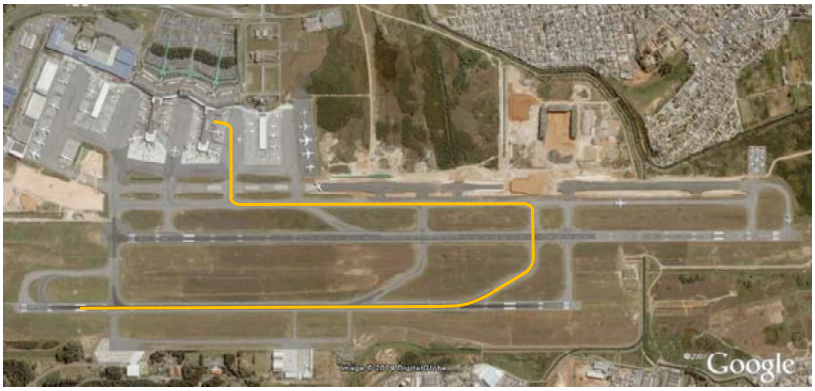

Figure 9 - *Cumbica* airport

Controller output was connected to the input to propulsion / brakes blocks. Two points need to be remembered: propulsion and brakes were defined in such a way that the actuation of both at the same time is not allowed and control signals are limited between *[0,1]*. Due to these considerations, the control input for brake / propulsion needed to be calculated in different ways, otherwise no valid control signal would be generated. The final form of the controller is provided by Fig. 10.

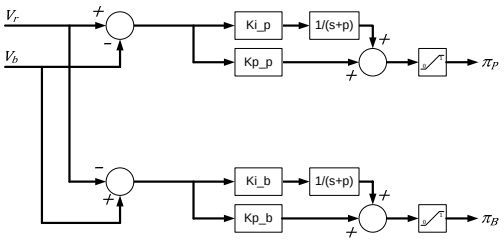

Figure 10 - Controller final form

3.1. Gain Determination

Once the control law was defined, gains were evaluated through an algorithm design technique. Using an optimization algorithm (*Matlab / Simulink Pattern Search*), the gains and poles of both control laws were changed to minimize the value of an objective function, defined in this study as a modified ITAE error, according to Eq. (28).

$$ITAE = \frac{\int_0^{tf} t \cdot |e(t)| dt}{t_f} \qquad (28)$$

The final values for controller parameters are provided by Tab. 4:

Kp_P	Ki_P	Kp_B	Ki_B	p_P	p_B
0,9375	0,3000	0,9625	0,9625	0	0,1875

Table 4 - Final values for controller parameters

4. SIMULATIONS AND RESULTS

With the gains evaluated, a simulation was performed to check the speed tracking. A typical speed profile was applied along the time to the model, with initial value of 72,0222 m/s (140 knot) and final value zero. The controller was exercised to provide the adequate tracking.

Figure 11 and Fig. 12 provide the final response and some interest signals.

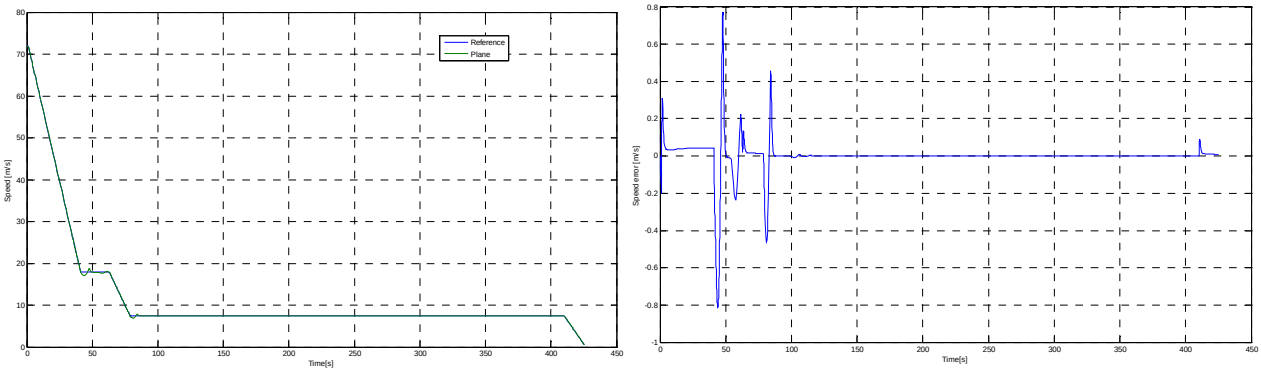

Figure 11 - Reference speed and aircraft speed / speed error

Observing Fig. 11, it can be noticed that the response was outstanding, occurring some small oscillation during the transitions (decelerations changes). The maximum error was less than 1 m/s, an acceptable value.

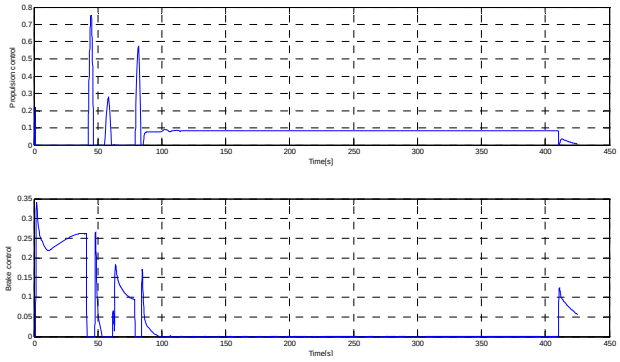

Figure 12 - Control signals

Figure 12 provides a good view of the control signals applied to the aircraft. The first point noticed is the range of the signals: both kept inside the interval [0,1], being fully compatible with the input range for brakes / engines. As expected, propulsion signal was kept to a minimum (just enough to compensate free wheel friction) during most of the time, when aircraft speed should be kept constant. Brakes were applied at the right moments, providing the good tracking even in speed changes (interval between 0-40s).

5. CONCLUSIONS

A mathematical model was developed for aircraft in ground situation. Landing gear, tires, brakes, propulsion and aerodynamics were taken into account, based on physical equation and data obtained from literature. The final model contains almost all components that generate efforts during landing run.

A simple control law was developed to track speed through the use of brakes and propulsion, using algorithm techniques to calculate the parameters of the control laws.

A typical speed profile was applied to the aircraft and a good response was obtained, with speed being tracked in a suitable way during all the time.

6. REFERENCES

Agência nacional de aviação civil, 2009, "Especificação de tipo nº EA-2003T05". São José dos Campos, 23 p.

Coetzee, E., Krauskopf, B. and Lowenberg, M., 2006, "Nonlinear Aircraft Ground Dynamics". International Conference on Nonlinear Problems in Aviation and Aerospace/

Currey, N. S., 1988, "Aircraft landing gear deisgn: principles and practices", American Institute of Aeronautics and Astronautics Inc., Washington D.C.

Duprez, J., Mora-Camino, F. and Vilaumé, F., June14-18, 2004, "Aircraft-on-ground Lateral Control for Low Speed Manuevers", 16th IFAC Symposium on Automatic Control in Aerospace, St. Petersburg, Russia.

Duprez, J., Mora-Camino, F., and Vilaumé, F., 2004, "Robust Control of the Aircraft-on-ground Lateral Motion". ICAS.

Embraer, 2008, "Airport planning manual - Section 02", May 25th, 2009, http://www.embraercommercialjets.com.br/english/content/ejets/emb_170.asp?tela=apm.

Etkin, B. and Reid, L. D., 1996, "Dynamics of flight - Stability and control", John Wiley & Sons Inc.

Goto K., Miyazawa, Y. and Sagisaka, M., August 6-9, 2001, "Development of Ground Taxiing Control Law for Automatic Landing Flight Experiment (ALFLEX)", AIAA Guidance, Navigation and Control Conference and Exhibit, Montreal, Canada.

Raymer, D. P., 2001, "Aircraft design: a conceptual approach", American Institute of Aeronautics and Astronautics Inc, Washington D.C.

Roskam, J., 2000, "Airplane design", DAR Corporation, Lawrence.

Yaeger J. T., Stubbs, M. S. and Davis, A. P., 1990, "Aircraft Radial-Belted Tire Evaluation", Nasa Langley Research Center, Hampton, VA.

7. RESPONSIBILITY NOTICE

The authors are the only responsible for the printed material included in this paper.